Empirical Validation of Low-Temperature PVT Collector for Heat Pump Integration

Francisco Beltrán, Nelson Sommerfeldt, Hatef Madani

KTH Royal Institute of Technology, Stockholm (Sweden)

Abstract

The combination of solar photovoltaic-hybrid (PVT) and ground source heat pumps (GSHP) can be a promising pathway towards the decarbonization of heating, cooling and electricity production in buildings. However, the concept of combining both technologies is still at an early stage in commercialization. As part of an ongoing 4-year research project, numerical modelling techniques have been applied to develop a digitally optimized PVT collector prototype specifically designed for heat pump integration. The goal of this study is to validate such models with a commercially available finned PVT collector against empirical data, with experiments carried out at an outdoor laboratory in Stockholm. Thermal and electrical outputs are measured for a range of low inlet fluid temperatures with varying flow rate, ambient temperature, solar irradiance and wind speed. R^2 values of 0.99 and 0.89 for electrical and thermal output respectively, show that the numerical model can predict real world performance of the collector with a high degree of certainty. The performance results show that the studied finned PVT collector has the potential to generate 800 W/m^2 of thermal power for a temperature difference of 30 K between inlet and ambient, and a solar irradiation of 1000 W/m^2. Even at a low irradiance of 200 W/m^2, a specific thermal output of 350 W/m^2 can be achieved, for a difference between inlet and ambient temperatures of 20 K.

Keywords: *Solar PV/thermal, PVT collector, Solar Heat Pump, COMSOL, Numerical Modelling*

1. Introduction and Background

A promising pathway to the electrification and decarbonization of buildings are solar heat pumps (SHP). There are numerous methods for combining the two technologies; however, one increasingly interesting approach is the series integration of photovoltaic/thermal hybrid collectors with ground source heat pumps (Kamel et al., 2015; Sommerfeldt and Madani, 2017). The design allows for shorter borehole lengths (Bertram et al., 2012), and in larger buildings with multiple boreholes, spacing reductions can reduce land requirements by up to 87% (Sommerfeldt and Madani, 2019). PVT also has the potential to regenerate degraded boreholes in older heat pump systems without the need for additional drilling. In addition, the operating temperatures in the borehole circuit are relatively low (-10°C to +20°C), allowing for a higher PVT collector thermal and electrical efficiency, and reduces costs by removing the need for glazing or insulation on the backside. Additionally, the electrical gains from lower PV cell temperatures is enough to cover the additional pumping power, making the additional thermal gains energetically free (Sommerfeldt and Madani, 2019; Vittorini et al., 2017).

When compared to solar thermal, the PVT+GSHP concept is relatively undeveloped and thus has had little design dedicated to PVT collectors as part of a heat pump system. When the thermal gains come from the solar collector and the surrounding air, the cost-benefit balance can change meaning a comprehensive techno-economic analysis is needed to identify the improvement potential of the current design. Chhugani et al., (2021) and Schmidt et al., (2018) investigated the empirical performance of PVT collectors as a single source for a heat pump, highlighting the system performance benefits of this configuration.

A 4-year research project aims at advancing the development and commercialization of an integrated heating, cooling and electricity system solution for European buildings using solar PVT and GSHP technology. One of the work packages in this project consists of applying numerical modelling techniques to develop a digitally optimized PVT collector prototype specifically designed for heat pump integration. Several designs have been modeled and studied with particular focus on enhanced heat capture from the surrounding air. Mass and heat transfer mechanisms as well as fluid dynamics have been considered in numerical modelling tool Comsol Multiphysics. Model validation is a critical part of the prototype development, so it becomes necessary to validate the results obtained from the simulations with experimental data in outdoor laboratory conditions.

doi:10.18086/eurosun.2022.12.02 Available at http://proceedings.ises.org

2. Objective and Methodology

The aim of this study is twofold. Firstly, it attempts to validate the numerical model of an unglazed, uninsulated PVT collector prototype with fins, specifically designed for heat pump integration in low temperature applications. This is done by using the commercially available numerical modelling software COMSOL Multiphysics, and comparing the results with the data obtained from the experimental testing of the collector prototypes. Secondly, it aims at quantifying the performance of a finned PVT collector by presenting the thermal performance curves for different flow rates and solar irradiance levels.

The experiments are performed in an outdoor setting using various flow rates and inlet temperatures during several days in July and August 2022 in Stockholm, Sweden. This provides a suitable range of ambient temperatures and solar irradiance levels to match the range of reduced temperatures tested in the simulations. To control for dynamic conditions (e.g. wind speed), measurements are selected and discretized such that they represent a quasi-steady state for comparison to steady-state results from the numerical model. Hourly averages for 30 different empirical data points are considered for the validation of the model. Outlet fluid temperatures from the PVT collectors, as well as thermal output and electricity generation are monitored for the 14 PVT collector array. Thermal and electrical outputs are assumed to be evenly distributed between all the collectors of the array, so the measured data is divided by 14 to get the measured values for one PVT collector.

The following step is to build the numerical model, where it is necessary to manually adjust the unknown parameters, such as thermal resistance between PV and absorber or the convective heat transfer coefficient on front and rear sides of the PVT collector, so that they can fit the empirical data in the best possible way. The same boundary conditions as in the experiments are then used as input in the numerical model, where outlet temperature from the PVT and PV cell temperature are obtained. These parameters are then used to calculate the thermal power and electricity generation. Outlet fluid temperature, PV electricity production and thermal output are used as validation metrics; tested using mean absolute error (MAE), mean biased error (MBE), and coefficient of determination (R^2). The model that best fits the empirical data is then the one that minimizes the errors and gives the highest coefficient of determination. Finally, the performance curves of the PVT collector at different flow rates and solar irradiation levels is plotted against the reduced temperature difference, based results from the simulations of the numerical model.

3. Method

In order to meet the objectives, it is required to have an testing facility where the PVT collector prototypes can be evaluated, and a model in Comsol Multiphysics software. In the following sections both the testing facility and numerical model are described in detail.

3.1. Testing facility

Testing of the PVT collectors is performed at an outdoor laboratory facility, located on the roof of the Energy Technology Laboratory at KTH Royal Institute of Technology, in Stockholm, Sweden. It consists of two independent arrays of 14 PVT and 2 PVT collectors respectively, mounted on a south-facing roof with a tilt angle of 45°. For the purpose of this study, only the 14 PVT collector array is considered. The larger PVT array is made up of two subarrays connected in series, where each subarray has seven collectors connected in parallel, for a total of 14 PVT collectors. The heat transfer fluid in the PVTs is an ethylene glycol – water mixture with a volumetric ratio of 25/75. The fluid is temperature controlled using a domestic heat pump, enabling supply temperatures down to -5 °C during summer days. This is done by connecting the collector array to a 300 L cold-water storage tank, where the evaporator of a 3-12 kW variable speed ATLAS Thermia heat pump cools down the heat transfer fluid in the tank and generates the low temperatures required at the inlet of the PVT collectors. The maximum source temperature of the heat pump at the inlet of the evaporator is 20 °C, and the maximum heating capacity of 12 kW is achieved at B5/W35 and a compressor speed of 5300 rpm. The testing facility also includes a hot water storage tank and a 10 kW Alfa Laval air-water heat exchanger for heat dissipation. The PVT collector arrays and mechanical room can be seen in Fig. 1, and a flow chart of the system with its monitoring equipment can be seen in Fig. 2.

The PVT collectors have been provided by Swedish startup Solhybrid i Småland, and consist of a glass-to-glass PV module with an aluminium manifold mechanically pressed against the rear glass. Having glass on the backside of the PV panel, as opposed to conventional PV, allows for a greater contact with the heat exchanger and increases mechanical strength, at the expense of an increased thermal resistance (Sommerfeldt and Ollas, 2017). The

manifold has a trough that fits a 12 mm copper pipe, which is also mechanically fixed. Thermal grease is added between the rear glass and aluminium manifold, as well as between the pipe and the trough to improve the thermal contact between the different surfaces. The thermal absorber-exchanger consists of six aluminium manifold and copper pipe units, each 150 mm wide and 1600 mm long, and are connected in a traditional parallel/harp configuration.

Fig. 1. Testing facility with mechanical room (left) and PVT collectors (right)

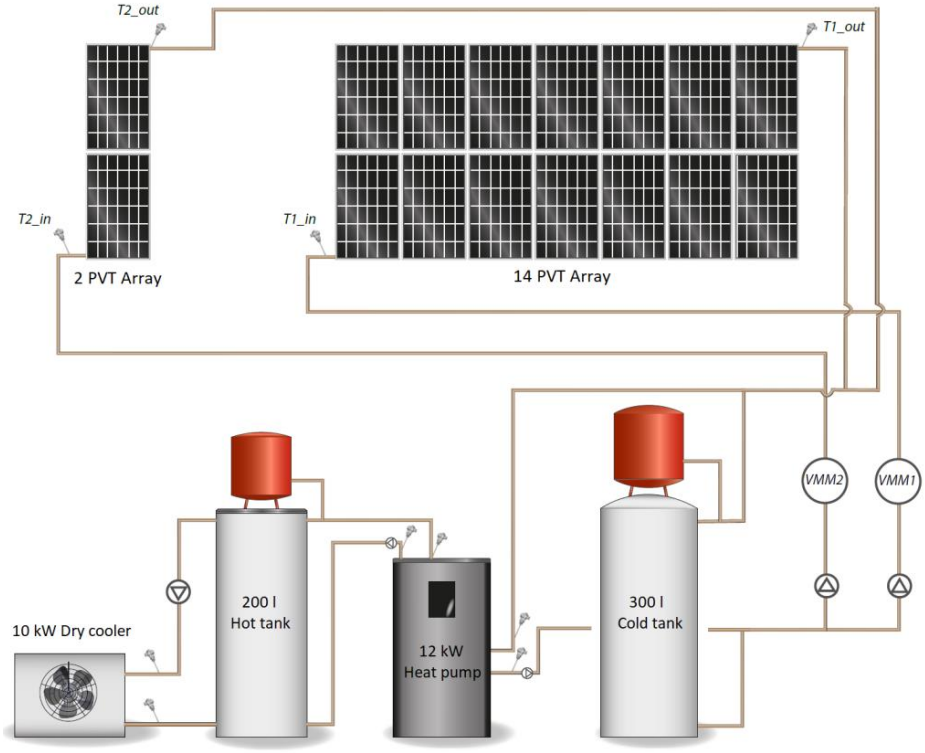

Fig. 2. System diagram with relevant measuring equipment

The PV module used for the PVT collectors is model PLM-285MA-60DG, a 60-monocrystalline-cells panel manufactured by Perlight Solar. The electrical ratings and specifications of the PV module are presented in Tab. 1. The conversion from the direct current (DC) generated by each module to alternating current (AC) is done by 14 Enphase IQ7 microinverters, one connected to each module.

Tab. 1. Electrical data of selected PV module

P_{max} (W_p)	Efficiency (η_{el})	Open-circuit voltage (V_{oc})	Short-circuit current (I_{sc})	Voltage at P_{max} (V_{mp})	Current at P_{max} (I_{mp})	Temp. coeff. P_{max} (β)
285 W	17.52 %	38.80 V	9.32 A	32.43 V	8.79 A	-0.40 %/K

A heat power meter is used to measure inlet and outlet temperatures to and from the PVT collectors, as well as flow rate and thermal power. In addition, a PT1000 temperature sensor is connected to the outlet of the PVT to

cross validate the measurements given by the heat meter. The entire system is monitored by two data loggers: one that tracks the electricity production from the microinverters, and one that tracks the heat pump performance, flow rates and the temperature levels within the system. The weather data is collected from a weather station installed directly above the PVT array, where ambient temperature, relative humidity, dew point, wind speed and direction are monitored. Solar irradiance is measured by a solar irradiance meter, located in the plane of the PVT collectors next to the array. All the measured data is obtained in 1-minute time steps, except for the electricity production that is measured every 5 minutes. A summary of the measurement equipment and the parameters that are being measured is presented in Tab. 2. Although there are other parameters that are being monitored in the system, such as compressor power or brine temperatures, only those relevant for this study are presented here.

Tab. 2. Measurement equipment and monitored parameters

Equipment	Quantity	Nomenclature
Weather Station	Ambient temperature (outdoor) [°C]	*T_amb*
	Wind speed [m/s]	*υ*
Solar irradiance meter	Incident solar irradiation [W/m^2]	*G*
Heat power meter (*VMM1* and *VMM2*)	Thermal power [W]	*Q_th*
	Volumetric flow rate [m^3/h]	*q*
	Inlet temperature to PVT [°C]	*T1_in & T2_in*
	Outlet temperature to PVT [°C]	*T1_out & T2_out*
Microinverters	Electrical power [W]	*P_el*

3.2. COMSOL model description

The PVT collector is modelled as a 1.6 x 0.9 m flat plate representing the glass-glass PV panel, and a metal thermal absorber with fins mechanically pressed to the back side. The PV panel consists of 5 layers: front glass, EVA encapsulate, silicon cells, EVA encapsulate, and rear glass, whereas the thermal absorber consists of the aluminum manifold and copper pipes that were described in the previous section. A thermal grease layer of 0.5 mm is added between the rear glass and aluminum manifold. To account for the imperfect thermal contact between the PV panel and absorber, the conductivity of the thermal grease that best fits the model is found to be 0.020 Wm^{-1}K^{-1} (thermal resistance of 0.017 m^{2}KW^{-1}) which is within the range of thermal resistance values of 0.010 – 0.040 m^{2}KW^{-1} found by Sommerfeldt and Ollas (2017) in their study of a similar collector. It is important to highlight that the thermal conductivity of the thermal grease also considers the imperfect bonding of absorber and PV, and consequent presence of air, which explains the low value. A summary of the material layers and properties is presented in Tab. 3, based on the study by Sommerfeldt and Ollas (2017).

Tab. 3. Material layers and properties

Layer	Material	Thickness [mm]	Density [kgm^{-3}]	Conductivity [Wm^{-1} K^{-1}]	Heat Capacity [Jkg^{-1}K^{-1}]
PV	Silicon	0.225	2330	148	677
EVA	EVA	0.5	960	0.7	2090
Glass	Glass	2.5	2530	1.8	500
Thermal grease	Thermal grease	0.5	2600[c]	0.02	1100[c]
Absorber plate	Aluminum	~ 1.75	2690[a]	218[a]	900[a]
Tube	Copper	1	8954	390	383
Fluid	Ethylene glycol - water	-	Vary w/temp	0.6	4186

[a] ASM International Handbook Committee, 1990

[b] Cristofari et al., 2009

[c] (Thermal Management, n.d.)

In order to reduce the required computational time and take advantage of the fact that the absorber consists of six identical and symmetrical manifold-pipe units, only one sixth of the PVT collector is modelled in COMSOL Multiphysics. An even flow distribution among all pipes and all collectors in the system is considered. A cross sectional diagram of PVT collector can be seen in Fig. 3.

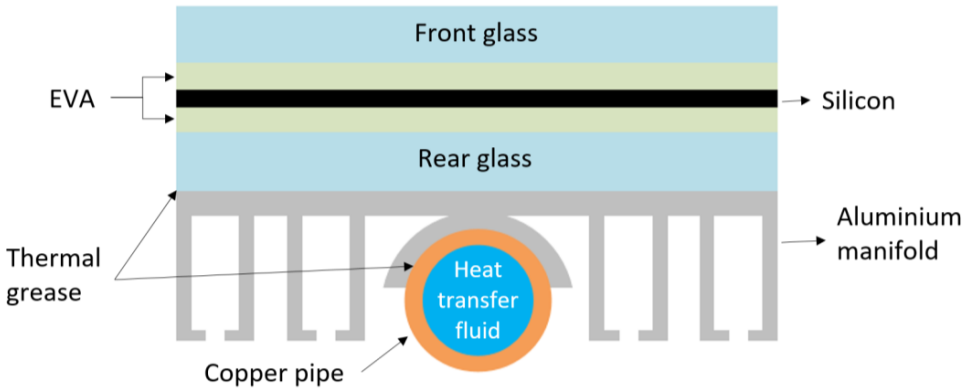

Fig. 3. Cross sectional diagram of the modeled PVT collector

Since the fluid flow falls in the laminar regime for all the measured flow rates, both laminar flow and heat transfer in solid and fluids interfaces with a non-isothermal flow multiphysics coupling are set up in COMSOL Multiphysics software. The PV part of the collector is modeled using a simple efficiency approach, where the electrical efficiency (η_{el}) is given by equation $\eta_{el} = \eta_0 \times [1 - \beta_0(T_{PV} - T_{ref})]$, being η_0 the efficiency of the PV cell at a reference temperature T_{ref}, T_{PV} the actual temperature of the PV cell, and β_0 the factor that governs the temperature dependence. The transmittance-absorptance factor is set at 0.81 (Sakellariou and Axaopoulos, 2018; Simonetti et al., 2018), whereas the sky temperature (T_{sky}) is given by expression $T_{sky} = 0.0552 \times T_{amb}^{1.5}$ (Duffie and Beckman, 1991).

The effect of wind speed on heat losses is a significant factor for unglazed PVT collectors (Sandnes and Rekstad, 2002). There are several methods to calculate the convective heat transfer coefficient in relation to wind speeds presented in the literature, but the model that best suits this case is a combination between the one presented by Cristofari et al., 2009 on the rear side of the collector, and the one presented by Watmuff et al., 1977 on the front side of the collector. According to Cristofari et al., 2009 , the convective heat transfer coefficient (h_c) with ambient air depends on whether the subject surface is on windward or leeward side and can be expressed by $h_c = 11.4 + 5.7\upsilon$ $Wm^{-2}K^{-1}$ and $h_c = 5.7$ $Wm^{-2}K^{-1}$ respectively. In this case, the rear side of the collector is considered to be on leeward, since for most of the hours in the period of study the wind is coming from the south or southwest directions. Thus, h_c is set at 5.7 $Wm^{-2}K^{-1}$. The convective heat transfer coefficient model on the front side of the collector is set at by $h_c = 2.8+3\upsilon$ $Wm^{-2}K^{-1}$ (Watmuff et al., 1977). The reason why a lower h_c might fit the model better than the higher one presented by Cristofari et al., 2009, is because of the effect of the full collector array as compared to a single collector. Frost formation, condensation gains and nighttime operation are not considered in the model.

In the testing facility there are two subarrays connected in series and each subarray has seven collectors connected in parallel. Assuming that the volumetric flow rate is evenly distributed between the PVT collectors in the array, the flow rate through each collector is calculated as 1/7 of the total volumetric flow rate into the array. Since the outlet temperature is measured at the end of the second subarray, the simulation is performed in two stages: the temperature at the outlet of the first PVT collector is obtained from the simulations, and it is used as inlet temperature for the second simulation. The results obtained from this second simulation is the one used for the calculation of the thermal output, which is then divided by two in order to calculate the value per module.

3.3. Performance evaluation

The performance of the PVT collectors is evaluated using three metrics:

- Thermal output (*Q_th)* in W for model validation
- Electrical output *(P_el)* in W for model validation
- Specific thermal output (q_th) in W/m^2 for the evaluation of the performance curves

When evaluating the thermal performance of the PVT collector for different flow rates and solar irradiation levels, the specific thermal output is plotted against the reduced temperature difference, defined as $T_{red} = (T_i - T_a)/G$ where T_i is the inlet temperature to the collector, T_a the ambient temperature, and G the solar irradiation.

To evaluate how well the numerical model fits the empirical data, three different statistical measures are used. Firstly, the Mean Absolute Error (MAE), which is calculated as the sum of the absolute errors divided by the

number of observations or data points, representing the average of the absolute errors. The expression for the calculation of MAE can be seen in (eq.1), where n is the number of observations, $\hat{y}_i$ is the simulated or predicted value and y_i the measured value.

$$MAE = \frac{1}{n}\sum_{i=1}^{n}|\hat{y}_i - y_i| \qquad \text{(eq. 1)}$$

Another statistical method used for the validation of the model is the Mean Biased Error (MBE), which is used to estimate the average bias in the prediction made by the model. A positive MBE means that the model is overestimating the dataset, whereas a negative MBE means that the model is underestimating the dataset. The expression for the calculation of MBE can be seen (eq.2).

$$MBE = \frac{1}{n}\sum_{i=1}^{n}(\hat{y}_i - y_i) \qquad \text{(eq. 2)}$$

The coefficient of determination (R^2) is the final statistical method to evaluate the accuracy of the model with regards to the measured data. It compares the variance of the dependent variable with the total variance. In other words, it helps to understand how differences in the dependent variable (simulation results), can be explained by the differences in a second variable. It shows how strong a linear relationship is between two variables, and is represented with a number between 0 (fails to explain variance) and 1 (fully explains variance). It can be calculated with (eq.3), where RSS is the sum of the squares of residuals, TSS the total sum of squares, and $\bar{y}$ the mean of the observed or measured data.

$$R^2 = 1 - \frac{RSS}{TSS} = 1 - \frac{\sum_i (y_i - \hat{y}_i)^2}{\sum_i (y_i - \bar{y})^2} \qquad \text{(eq. 3)}$$

4. Results

Of all the data gathered, 30 different hours of measurements are selected, based on the requirement that there should be 60 sequential measurements with a determined level of variance for each of the different measured parameters. If that condition is met, then it is assumed that the conditions are steady state for that hour, and it is then used as a single data point. The level of variance is determined by the Coefficient of Variation (CV), which is defined as the standard deviation divided by the mean of the sample. The acceptable CV for each of the input parameters is presented in Tab. 4.

Tab. 4. Acceptable coefficient of variation for measured parameters

Parameter	Acceptable CV
Volumetric flow rate	<10%
Inlet temperature	<10%
Ambient temperature	<10%
Solar irradiance	<30%

Although the original idea was to have a low variability of wind speed measurements, this was deemed impossible. However, the collectors have a relatively high thermal inertia, so the variance in wind speeds should have a minimal impact on the fluid temperatures (Sommerfeldt and Ollas, 2017).

Tab. 5 shows the values for the different boundary conditions. The range of measured ambient temperatures in the 30-point data set was between 13 °C and 24 °C, with an even frequency distribution along the range. Inlet temperatures varied between 1 °C and 12 °C, with 40 % of the measurements occurring between 6 °C and 8 °C. When looking at solar irradiation levels, almost half of the data points were below 400 W/m^2, however, 20 % of them were over 800 W/m^2. The variation of average wind speeds was in the range of 0 to 7 m/s, with a quite even distribution along the range. Volumetric flow rate varied was mostly around 80 lh^{-1}m^{-2}, with a few experiments performed at lower values.

The measured values of ambient temperature, inlet temperature, solar irradiance, wind speed and flow rate are used as inputs in the COMSOL model, where outlet temperature and average PV cell temperatures are obtained as outputs. Outlet fluid temperature is then used to calculate the thermal output of the PVT collector and thermal efficiency, whereas the average PV cell temperature is used to calculate the specific electrical output and the electrical efficiency.

Tab. 5. Measured values of boundary conditions

Flow rate [$lh^{-1}m^{-2}$]	Inlet Temp. [°C]	Ambient Temp. [°C]	Solar irradiance [W/m^2]	Wind speed [m/s]
81.4	6.13	24.23	73.0	4.7
81.2	5.89	22.83	23.5	4.5
81.8	6.50	21.89	300.2	4.6
79.5	5.80	19.76	142.9	6.7
82.1	6.77	19.42	712.5	6.3
27.2	5.59	19.28	0.0	3.4
44.2	5.36	16.53	46.3	2.6
30.3	5.36	18.36	0.0	1.6
30.4	4.80	16.99	0.0	2.6
81.2	5.88	20.11	274.3	5.0
81.1	5.83	20.15	191.7	5.3
34.7	5.33	17.30	83.2	2.5
39.0	6.21	16.68	42.5	1.5
82.8	7.63	16.85	450.7	6.4
82.5	7.48	18.51	53.5	6.7
84.6	8.31	18.24	256.4	4.4
27.9	5.74	18.19	0.0	1.3
82.7	8.16	13.48	221.9	0.3
74.7	7.69	15.58	174.8	0.8
43.8	7.31	14.44	66.2	0.0
85.3	9.89	18.21	1021.7	2.8
86.5	11.41	20.84	945.8	5.1
86.2	10.99	20.49	857.5	4.2
66.8	1.78	21.21	491.0	1.9
81.9	6.29	20.70	542.0	6.8
82.0	6.83	20.15	671.9	5.2
78.7	8.48	13.48	545.7	0.5
83.9	9.33	16.87	882.9	2.4
88.5	11.03	18.93	693.6	5.2
85.8	11.09	19.90	887.5	5.6

4.1. Model validation

Fig. 4 shows the measured values of outlet temperature on the x-axis, and the simulated values of the outlet temperature in the y-axis. It can be seen that the different data points are scattered close to the y=x line with a few exceptions. The model seems to be overestimating the outlet temperatures for lower values, and underestimating it for higher ones. The maximum absolute error is around 2.5 K, but the mean absolute error is considerably lower, with a value 0.70 K. A mean biased error of 0.16 K shows that the model is slightly overestimating the outlet temperature of the PVT collectors, but the value is low to consider it a problem. Finally, a coefficient of determination of 0.902 shows that more than 90 % of the variability in the simulated results of the outlet temperature can be explained by the variability in the measured data, which means that the model can represent real world performance accurately.

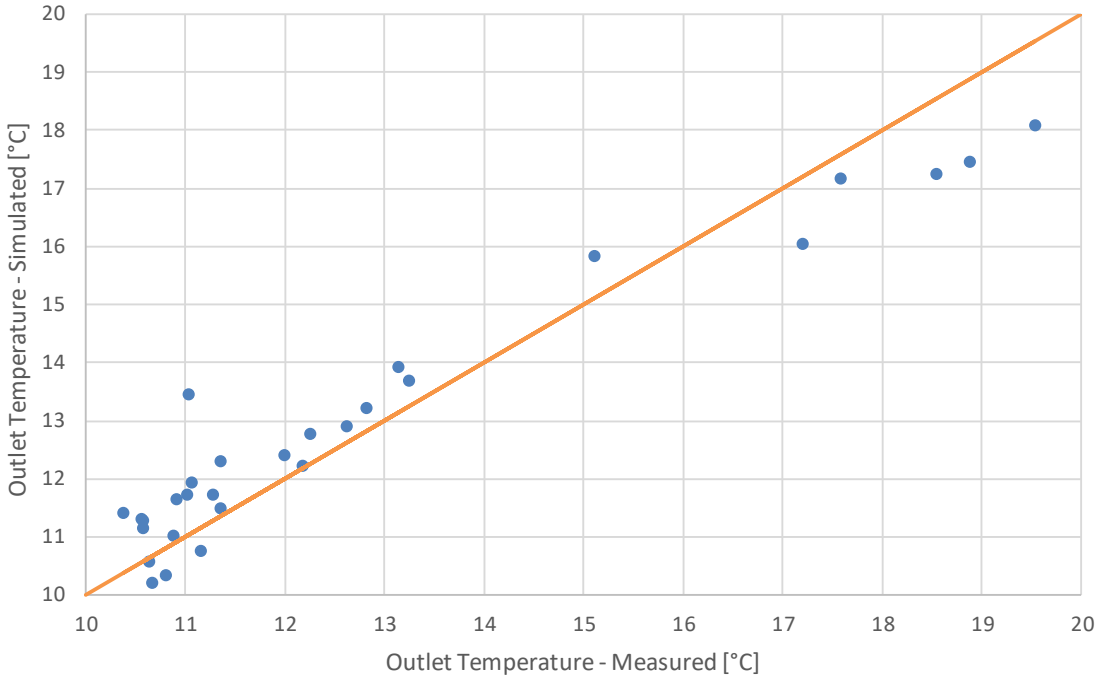

Fig. 4. Simulated outlet temperature values plotted against measured outlet temperature values

Fig. 5 shows the measured values of thermal output obtained from the heat meters on the y-axis, against the thermal output calculated with the simulation results. Once again it can be seen that the data points are scattered close to the y=x line, with the highest absolute errors occuring for the highest values of thermal output. The maximum absolute error is close to 150 W, represeting a relative difference of 25 %. However, the mean absolute error is almost four times smaller. When calculating the mean biased error, the result of 4.5 W shows that the model is overestimating the thermal power production, which is alligned with the results obtained for the outlet temperature. A coefficient of determination of 0.89, shows a good relationship between real world performance and the simulated results.

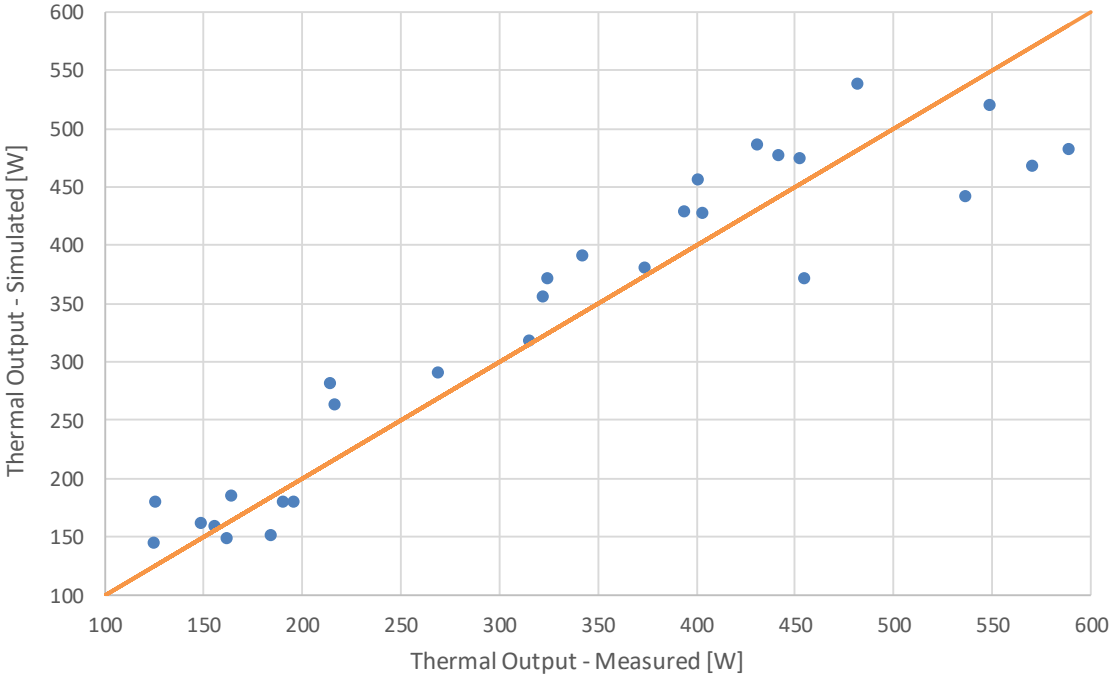

Fig. 5. Simulated thermal output values plotted against measured thermal output values

Fig. 6 shows the measured values of electrical output obtained from the microinverters on the y-axis, against the electrical output from the simulation results, using a simple efficiency approach. It can be seen that most of the

data points are close to the y=x lines, with the highest absolute errors of approximately 25 W and relative error of 10 % occurring when the electricity production is the highest. For low electricity production values, the simple efficiency approach fits the measured values precisely. A MAE of 4.20 W, a MBE of 0.48 W, and R^2 value of 0.995, shows that the simple efficiency approach can predict the electricity production from each collector in a good way.

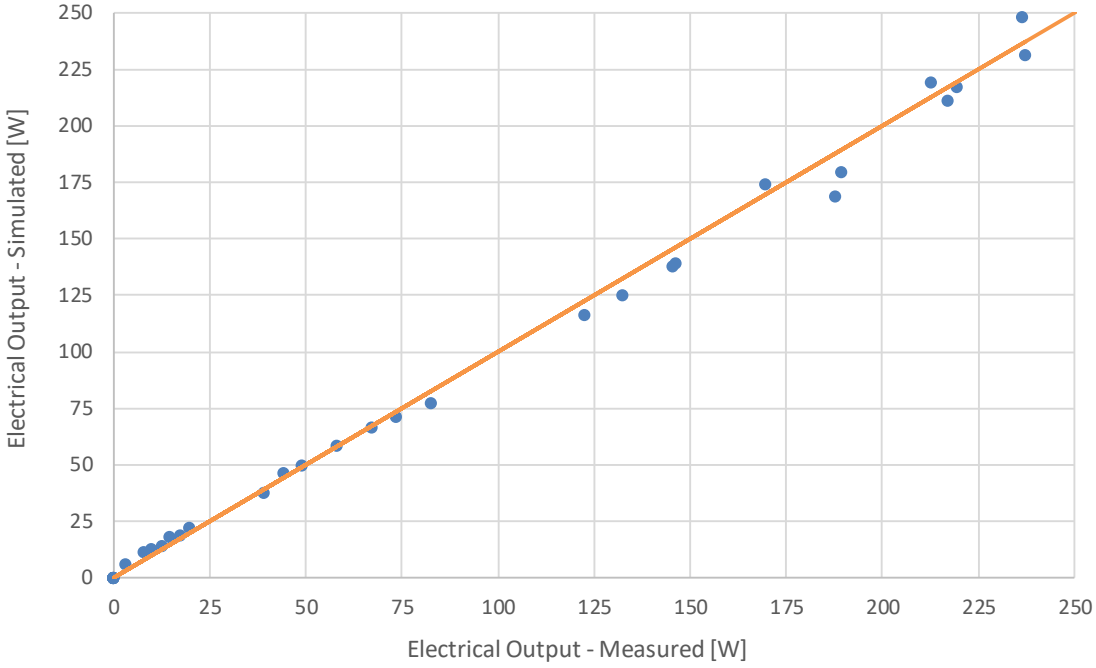

Fig. 6. Simulated electrical output values plotted against measured electrical output values

The statistical methods results for outlet temperature, thermal power and electrical power can be seen in Tab. 6.

Tab. 6. Statistical methods summary of results

	Temperature Out	Thermal Power	Electrical Power
Mean Absolute Error (MAE)	0.70 K	40.02 W	4.20 W
Mean Biased Error (MBE)	0.16 K	4.48 W	-0.48 W
Coefficient of Determination (R^2)	0.902	0.887	0.995

4.2. Performance curves

This section presents the performance curves of the studied PVT collector for different solar irradiation levels and flow rates based on the numerical modelling results. Ambient temperature is fixed at 20 °C and wind speed at 1 m/s. For the evaluation of the performance of the PVT collectors under different solar irradiation levels, a constant flow rate of 80 $lh^{-1}m^{-2}$ is considered. The results in Fig. 7 show that even when the solar irradiance is as low as 200 W/m^2, thermal output can be as high as 530 W/m^2 or 363 W/m^2 for reduced temperature differences of -0.15 Km^2W^{-1} and -0.10 Km^2W^{-1} respectively. As would be expected, the maximum thermal output occurs when solar irradiation is 1000 W/m^2 with a reduced temperature difference of -0.03 Km^2W^{-1}, which is equivalent to a temperature difference between ambient and inlet to the collector of 30 K. For this case, the specific thermal output can be as high as 800 W/m^2 or 1160 W/collector. The performance at a reduced temperature difference of 0 Km^2W^{-1}, varies between 26.1 W/m^2 for the lowest solar irradiation case, and 297.7 W/m^2 for the highest solar irradiation case.

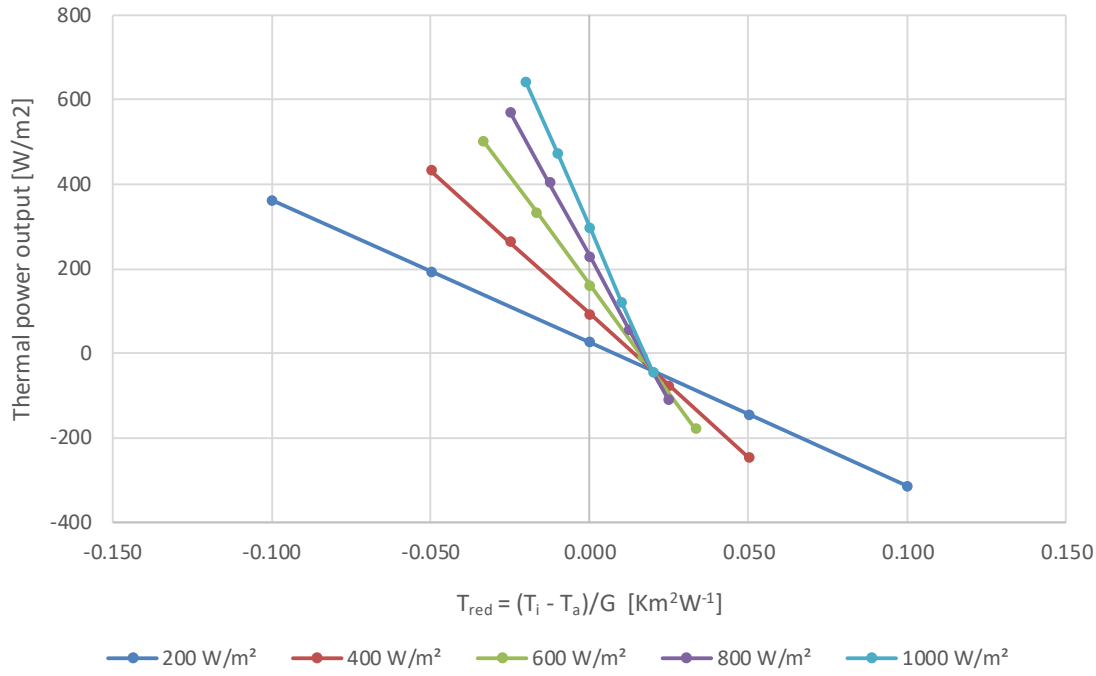

Fig. 7. Thermal performance curve of PVT collector prototype obtained from Comsol Multiphysics simulations

For the evaluation of the performance of the PVT collectors under different volumetric flow rates, a constant solar irradiation level of 1000 W/m^2 is considered. The results in Fig. 8 show that increasing the flow rate from 20 lh^{-1}m^{-2} to 100 lh^{-1}m^{-2} has diminishing returns. For a reduced temperature difference of -0.02 Km^{2}W^{-1}, increasing the flow rate from 20 lh^{-1}m^{-2} to 40 lh^{-1}m^{-2}, increases thermal output from 414.7 W/m^2 to 519.5 W/m^2, equivalent to 25.3 %. However, when flow rate is further increased to 60 lh^{-1}m^{-2}, 80 lh^{-1}m^{-2} and 100 lh^{-1}m^{-2}, the increase in specific thermal output is of 13.2 %, 9.3 % and 7.1 %. The performance at a reduced temperature difference of 0 Km^{2}W^{-1}, varies between 193 W/m^2 for a flow rate of 20 lh^{-1}m^{-2}, and 318.6 W/m^2 for 100 lh^{-1}m^{-2}, which is a lower variation than what occurs for the one occurring for the different solar irradiation levels. It is worth noting that the flow remains always in the laminar regime, with a Reynolds number of 450 at 100 lh^{-1}m^{-2}.

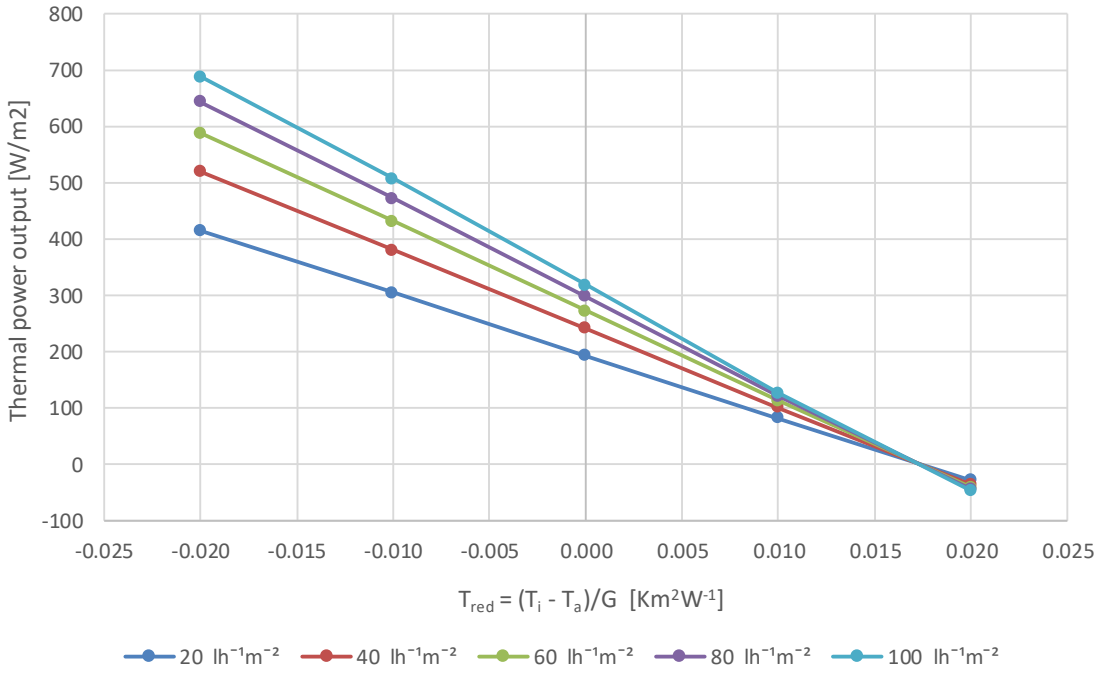

Fig. 8. Thermal performance curve of PVT collector prototype obtained from Comsol Multiphysics simulations

5. Discussion and Conclusions

The analysis presented in this paper shows that the numerical model of a sheet and tube PVT collector with fins specifically designed for heat pump integration, fits the empirical data with an R^2 value of more than 88% for the main three output parameters: outlet temperature, thermal output and electrical output. However, the MAE for outlet temperature and thermal power needs to be discussed further.

To begin, the thermal output of the full collector array was measured in the experiments and divided by 14 to calculate the value for one collector, but in the model only two collectors were considered. All collectors were assumed to generate the same amount of power, although most probably the subarray that has the lowest inlet temperature produces a higher thermal output than the following subarray, due to a higher temperature difference between inlet temperatures and ambient, enhancing the heat capture from the surrounding air. While this may be a limitation in validating a single collector, since it is expected that PVT will nearly always be installed in an array, the approach used here captures variance between individual collectors that can be missed if only using a single sample.

Condensation effects were not considered in this study, which could be an important issue when the difference between inlet temperature and dew point temperature is high. However during the experiments, no considerable amount of condensation was observed on the rear side of the PVT collectors, so it was not considered to be a critical modelling aspect for the studied data range.

It is important to highlight that even though the highest thermal output obtained from the measurements was 368 W/m^2, based on the performance curves obtained from the simulations of the validated numerical model, the thermal output of the sheet and tube PVT collector with fins could more than double that value. This can happen for example, when there is a brine temperature coming out of the borehole field below -5 °C, there is an ambient temperature of 25 °C and the solar irradiance is 1000 W/m^2. Although not a common scenario, this could be possible and helps set an upper limit for the amount of heat that can be extracted from the collector. However, even at low irradiation levels, the PVT collector can work mostly as an air-water heat exchanger achieving a specific thermal output of more than 300 W/m^2. In a study currently under peer-review, the addition of fins are shown to increase heat capture from the air by up to 60 % over unfinned designs.

The finned design is still relatively unique and a developing segment of PVT design. This work builds on the body of knowledge that defines the performance and potential of PVT heat pumps systems by describing an empirically validated numerical model. Further work in finned PVT collector development and analytical models in full systems analysis (e.g. TRNSYS) can be informed using COMSOL, reducing time and effort. Future work will quantify the full PVT+HP system performance and the benefits finned collectors provide.

6. References

ASM International Handbook Committee, 1990. ASM Handbook, Volume 02 - Properties and Selection: Nonferrous Alloys and Special-Purpose Materials. ASM International.

Bertram, E., Glembin, J., Rockendorf, G., 2012. Unglazed PVT collectors as additional heat source in heat pump systems with borehole heat exchanger. Energy Procedia 30, 414–423. https://doi.org/10.1016/j.egypro.2012.11.049

Chhugani, B., Pärisch, P., Kirchner, M., Littwin, M., Lampe, C., Giovannetti, F., 2021. Model Validation and Performance Assessment of Unglazed Photovoltaic-Thermal Collectors with Heat Pump Systems 1–12. https://doi.org/10.18086/eurosun.2020.05.13

Cristofari, C., Notton, G., Canaletti, J., 2009. Thermal behavior of a copolymer PV/Th solar system in low flow rate conditions. Sol. Energy 83, 1123–1138. https://doi.org/10.1016/j.solener.2009.01.008

Duffie, J.A., Beckman, W.A., 1991. Solar Engineering of Thermal Processes.

Kamel, R.S., Fung, A.S., Dash, P.R.H., 2015. Solar systems and their integration with heat pumps: A review. Energy Build. https://doi.org/10.1016/j.enbuild.2014.11.030

Sakellariou, E., Axaopoulos, P., 2018. An experimentally validated, transient model for sheet and tube PVT collector. Sol. Energy 174, 709–718. https://doi.org/10.1016/j.solener.2018.09.058

Schmidt, C., Schäfer, A., Kramer, K., 2018. Single source "solar thermal" heat pump for residential heat supply: Performance with an array of unglazed PVT collectors, in: 12th ISES Eurosun Conference. Rapperswil, Switzerland.

Simonetti, R., Molinaroli, L., Manzolini, G., 2018. Development and validation of a comprehensive dynamic mathematical model for hybrid PV/T solar collectors. Appl. Therm. Eng. 133, 543–554. https://doi.org/10.1016/j.applthermaleng.2018.01.093

Sommerfeldt, N., Madani, H., 2019. In-depth techno-economic analysis of PV/Thermal plus ground source heat

pump systems for multi-family houses in a heating dominated climate. Sol. Energy 190, 44–62. https://doi.org/10.1016/j.solener.2019.07.080

Sommerfeldt, N., Madani, H., 2017. Review of Solar PV/Thermal Plus Ground Source Heat Pump Systems for European Multi-Family Houses 1–12. https://doi.org/10.18086/eurosun.2016.08.15

Sommerfeldt, N., Ollas, P., 2017. Reverse engineering prototype solar pv/thermal collector properties from empirical data for use in TRNSYS Type 560. ISES Sol. World Congr. 2017 - IEA SHC Int. Conf. Sol. Heat. Cool. Build. Ind. 2017, Proc. 1121–1132. https://doi.org/10.18086/swc.2017.18.11

Thermal Management, n.d. Thermal Pastes [WWW Document]. Therm. Manag. URL https://www.thermalmgt.com/thermal-pastes/ (accessed 9.10.22).

Vittorini, D., Castellucci, N., Cipollone, R., 2017. Heat recovery potential and electrical performances in-field investigation on a hybrid PVT module. Appl. Energy 205, 44–56. https://doi.org/10.1016/j.apenergy.2017.07.117

Watmuff, J., Proctor, D., Australia, S., 1977. Solar and wind induced external coefficients-Solar collectors. COMPLES.